Paper

THERMAL RESPONSE OF HUMAN SKIN TO MICROWAVE ENERGY: A CRITICAL REVIEW

Kenneth R. Foster,* Marvin C. Ziskin,† and Quirino Balzano‡

Abstract—**This is a review/modeling study of heating of tissue by microwave energy in the frequency range from 3 GHz through the millimeter frequency range (30–300 GHz). The literature was reviewed to identify studies that reported RF-induced increases in skin temperature. A simple thermal model, based on a simplified form of Pennes' bioheat equation (BHTE), was developed, using parameter values taken from the literature with no further adjustment. The predictions of the model were in excellent agreement with available data. A parametric analysis of the model shows that there are two heating regimes with different dominant mechanisms of heat transfer. For small irradiated areas (less than about 0.5–1 cm in radius) the temperature increase at the skin surface is chiefly limited by conduction of heat into deeper tissue layers, while for larger irradiated areas, the steady-state temperature increase is limited by convective cooling by blood perfusion. The results support the use of this simple thermal model to aid in the development and evaluation of RF safety limits at frequencies above 3 GHz and for millimeter waves, particularly when the irradiated area of skin is small. However, very limited thermal response data are available, particularly for exposures lasting more than a few minutes to areas of skin larger than 1–2 cm in diameter. The paper concludes with comments about possible uses and limitations of thermal modeling for setting exposure limits in the considered frequency range.**
Health Phys. 111(6):528–541; 2016

Key words: exposure, radiofrequency; microwaves; radiation, nonionizing; safety standards

INTRODUCTION

Major international exposure limits for radiofrequency (RF) energy (nominally 3 kHz–300 GHz) have been in place for many years. These include IEEE C95.1-2005 and C95.1-2010 and the limits of the International Commission on Nonionizing Radiation Protection (ICNIRP 1998). These limits, together with U.S. limits of the Federal Communications Commission (FCC 2010), are all presently undergoing their periodic revision and updating. While these limits cover frequencies as high as 300 GHz, they have principally been based on studies involving exposures at or below the Industrial-Scientific-Medical (ISM) band at 2.45 GHz, where most applications of RF energy with significant potential for human exposure have heretofore resided. However, new technologies are emerging that will operate at higher frequencies and create new exposure situations. The next big advance in wireless communications will be 5G, which is anticipated to use what one author calls "vast amounts of relatively idle spectrum …in the mmWave [millimeter wave frequency] range of 30–300 GHz" (Andrews et al. 2014). This technology will deploy large numbers of low powered transmitters, with many intended to be used close to the body as with present mobile phones.

The immediate motivation of this work is the recent observation by Colombi et al. (2015) that technical features in these current exposure limits result in sharp and biologically unjustified transitions at 3, 6, or 10 GHz in the maximum allowed power that can be radiated from antennas placed close to the body. These transitions result from the shift in the guidelines from specific absorption rate (SAR) to power density as the quantity used for their basic restrictions, together with provisions of the guidelines for small-area exposure to the skin. While they have no biological basis, the transitions have significant potential impact on new communications devices including 5G wireless communications. A systematic analysis of RF hazard mechanisms from 3 GHz through the millimeter band would be useful to help resolve such issues and inform the development of improved exposure limits. Since the only recognized hazards of RF energy in this frequency range are associated with excessive heating, this calls for a useful theoretical model heating of tissue over a wide range of exposure frequency.

This present study (a) surveyed available data on heating of tissues with microwave energy at 3 GHz or above,

*Department of Bioengineering University of Pennsylvania, Philadelphia, PA; †Temple University Medical School, Philadelphia, PA; ‡Department of Electrical and Computer Engineering, University of Maryland, College Park, MD.

The authors declare no conflicts of interest.

For correspondence contact: Kenneth R. Foster, Department of Bioengineering, University of Pennsylvania, 240 Skirkanich Hall, 210 S. 33rd Street, Philadelphia, PA 19104, or email at **kfoster@seas.upenn.edu**.

(*Manuscript accepted* 18 *July* 2016)

0017-9078/16/0

DOI: 10.1097/HP.0000000000000571

including the millimeter-wave range from 30–300 GHz; (b) considered a simple thermal model and examined its scaling properties; and (c) compared the predictions of the model against the data. The model is based on a simplified form of Pennes' bioheat equation (BHTE) and is used without adjustment in parameters (Pennes 1948). While many alternative models for heat transfer in tissue have been proposed, some with stronger theoretical rationale (e.g., Xu et al. 2009; Bhowmik et al. 2013; Baish 2014), these models typically require detailed and location-specific information about vascular structure and consequently are difficult to apply. In addition, most have been subjected to only limited tests against experimental data (where often the data were used to fit the parameters of the models). The present approach is to take the simplest possible model and compare its results to existing data without post hoc adjustment of parameters.

METHODS

In simplified form, Pennes' bioheat equation (BHTE) can be written:

$$k\nabla^2 T - \rho^2 C_{m_b} T + \rho SAR = \rho C \frac{dT}{dT}, \qquad (1)$$

Where

T = the temperature rise of the tissue (°C) above the baseline temperature (i.e. temperature above that previous to RF exposure);

k = the thermal conductivity of tissue (0.37 W m^{-1} °C^{-1});

SAR = the microwave power deposition rate (W kg^{-1});

C = the heat capacity of the tissue (3,390 W s kg^{-1} °C^{-1});

ρ is the tissue density (1,109 kg m^{-3}); and

m_b is the volumetric perfusion rate of blood [1.767 × 10^{-6} m^3/(kg s^{-1}) or 106 mL min^{-1} kg^{-1} in the mixed units typically used in the physiology literature].

It is noted that this formulation contains a number of drastic approximations (discussed below) and is presented as the simplest analytical expression that might be useful for comparison to data over a range of exposure conditions, rather than as an exact formulation of the heat transfer problem. However, Pennes' BHTE is the most widely used formulation of bioheat transfer (his 1948 paper has been cited more than 2,000 times according to the Web of Science). The parameter values in eqn (1) are those used by a commercial FDTD (finite difference time domain)/thermal analysis program that is widely used for RF exposure assessment (Hasgall et al. 2015) without further modification. Eqn (1) was solved numerically using a 2D finite element program (PDEase, Macsyma, Arlington, MA, USA) assuming insulated boundary conditions, a conservative assumption. This is justified because the rate of conduction of the heat from microwave exposure into deeper layers of skin can be expected to be well below the rate of heat loss from skin to the environment; i.e.,

$$k\frac{\partial T}{\partial z} > h(\Delta T_{sur} - T_{air}) \qquad (2)$$

where T_{sur} and T_{air} are the temperatures of the tissue surface and surrounding air, $\frac{\partial T}{\partial z}$ is the temperature gradient at the surface (of the order of hundreds of °C per meter) and h is a heat transfer coefficient that is of the order of 1–10 W m^{-1} °C (Fiala et al. 1999). Also, as discussed below, natural rates of heat transfer from the skin to the environment are of the order of a hundred W m^{-2}, whereas the microwave exposures considered here are generally an order of magnitude larger.

For plane wave RF energy normally incident on a uniform plane of tissue, the source term in eqn (1) can be written

$$SAR = \frac{I_o T_{tr}}{\rho L} e^{-z/L} \qquad (3)$$

where I_o is the incident power density on the tissue, T_{tr} is the energy transmission coefficient into the tissue, and L is the energy penetration depth into tissue, which is defined as the distance beneath the surface at which the SAR has fallen to a factor of 1/e below that at the surface. L is one-half of the more commonly reported wave penetration depth. T_{tr} and L are shown in Fig. 1 as a function of frequency, calculated using dielectric data from dry skin reported by Gabriel et al. (1996).

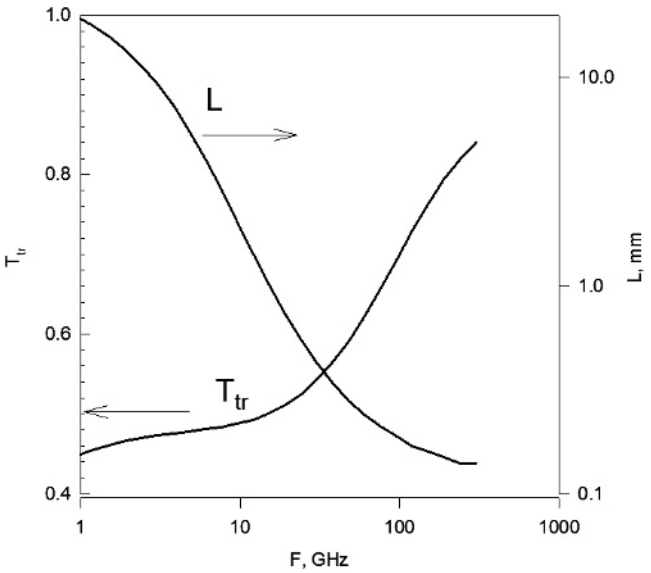

Fig. 1. Transmission coefficient (T_{tr}) and 1/e SAR penetration depth (L) for plane wave RF energy incident normally on skin, calculated using dielectric data for dry skin from Gabriel et al. (1996) [Electrical properties above 20 GHz extrapolated from data at lower frequencies; see Gabriel et al. (1996)].

Scaling properties of BHTE

The main focus of the present discussion is on the scaling properties of the BHTE equation; i.e., the variation of temperature increases with model parameters. This will be examined for two limiting cases.

1D model: semi-infinite plane exposed to incident plane wave. The thermal response of the one-dimensional (1D) model is characterized by two time scales representing heat transport by blood perfusion and thermal conduction, respectively:

$$\tau_1 = 1/m_b\rho \approx 500 \text{ sec} \qquad \tau_2 = L^2/\alpha \qquad (4\text{ a, b})$$

where $\alpha = k/\rho C$ is the thermal diffusivity (9.8×10^{-8} m^2 s^{-1}). These time constants are shown as a function of frequency in Fig. 2.

Analytical solutions to the BHTE for the 1D problem have been presented elsewhere in the time domain (e.g., Foster et al. 1978; Nelson et al. 2003); a Green's function for the equation is also available (Gao et al. 1995; Yeung and Atalar 2001). The solutions are cumbersome and are not repeated here in full form. Among many other studies that have employed the BHTE, a useful one-dimensional model that examines effects of parameter variation on the heating of skin by microwave energy but takes into account several layers of tissue (skin, fat, muscle), has been proposed by Kanezaki et al. (2010).

For low perfusion rates ($m_b \rightarrow 0$), eqn (1) approaches the simple heat conduction equation. In that case, the transient solution for the surface temperature T_{sur} is easily found:

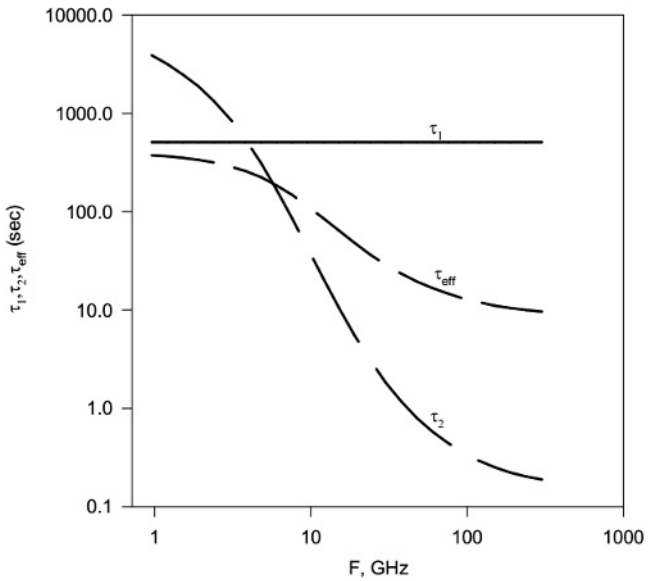

Fig. 2. Thermal time constants calculated using the model parameters assumed in this study (from eqns 3 a, b and 5b).

$$T_{sur}(t) = C_1\sqrt{t} - C_2\left(1 - e^{t/\tau_2} erfc\sqrt{t/\tau_2}\right)$$

where

$$C_1 = \frac{2I_oT_{tr}}{\sqrt{\pi k\rho C}} = 9.54 \times 10^{-4} I_oT_{tr} \ ^\circ C/\sec^{1/2} \qquad (5\text{ a, b, c})$$

$$C_2 = \frac{I_oT_{tr}L}{k} = 2.7 \times I_oTtr \ ^\circ C.$$

The first term to the right in eqn (5a) is the solution for the case of pure surface heating (corresponding to the limit $L \rightarrow 0$). The second term rapidly approaches zero as $t > \tau_2$ and describes an early transient effect associated with diffusion of heat over the energy penetration depth L. In the absence of a perfusion term in eqn (1), after an initial transient, T_{ss} increases without limit as $t^{1/2}$.

In the presence of blood flow ($m_b > 0$), T_{sur} approaches a steady-state value T_{ss} that can be written as the product of the SAR at the surface and an effective thermal time constant τ_{eff} (Foster et al. 1998):

$$T_{ss} = \frac{SAR_o}{C}\tau_{eff} \ (surface\ temperature,\ steady\ state)$$

where

$$\tau_{eff} = \frac{\tau_2 - \sqrt{\tau_1\tau_2}}{\tau_2/\tau_1 - 1} \qquad SAR_o = \frac{I_oT_{tr}}{\rho L}. \qquad (6\text{ a, b, c})$$

In the two limiting cases ($\tau_2 >> \tau 1$) and ($\tau_2 << \tau_1$), τ_{eff} approaches the asymptotic values of τ_1 and $(\tau_1\ \tau_2)^{1/2}$ respectively, and T_{ss} takes on the limiting values (for the 1D problem)

$$T_{ss} \rightarrow \frac{I_oT_{tr}}{\rho\sqrt{Cm_bk}} \quad \tau_1/\tau_2 \rightarrow \infty \qquad pt \rightarrow \frac{I_oT_{tr}}{LCm_b\rho^2} \quad \tau_1/\tau_2 \rightarrow 0. \qquad (7\text{ a, b})$$

Over most of the frequency range of present interest, $\tau_1 >> \tau_2$, and the steady state increase in temperature at the surface for the 1D case approaches eqn (7a), showing a modest dependence (as $m_b^{-1/2}$) on the blood perfusion term.

Fig. 3 shows the transient increase in surface temperature for an exposure at 6 GHz for several assumed values of m_b. The time axis is scaled as $t^{1/2}$ to show the the dominance of heat conduction at short times and the approach to the steady state at long times. At frequencies above 30 GHz, the thermal response is nearly independent of frequency and essentially the same as from purely surface heating.

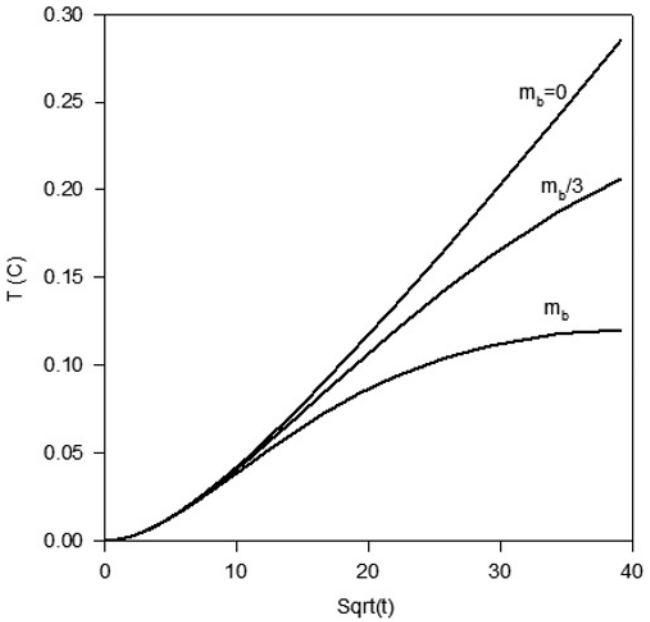

Fig. 3. Temperature increase at the surface (T_{ss}) for the plane model with $IoT_{tr} = 10$ W m^{-2} at 6 GHz, for a conduction-only model ($m_b = 0$), "normal" (m_b in eqn 1), and one-third "normal" blood perfusion. The abscissa is scaled as $t^{1/2}$ to highlight the late transient response of the 1D heat conduction problem (eqn 4a). Effects of blood perfusion are seen as the departure of the transient response from the $t^{1/2}$ behavior at > 100 s.

The scaling properties of the BHTE in the spatial domain can be investigated with reference to the Green's function for the equation (Yeung and Atalar 2001; Gao et al. 1995). The Green's function decays exponentially with distance with two intrinsic distance scales. Using the parameter values given above, these are

$$R_1 = \frac{\sqrt{k}}{\rho\sqrt{m_b c}} \approx 7\,\text{mm} \qquad (8\ \text{a, b})$$
$$R_2 = \sqrt{4\alpha t} \approx 0.5\sqrt{t}\,\text{mm sec}^{-1/2}$$

The first of these (R_1) accounts for the smoothing effect of blood perfusion. The second, R_2, is a measure of the distance that heat diffuses in time t. The temperature field is obtained by convolving the Green's function with the SAR pattern. Since convolution is a form of averaging, the temperature increase at any point can be described approximately as a volume average of the SAR pattern using a weighting function that decays rapidly with distance as the shorter of R_1 or R_2.

2D case: irradiated disk. Two subcases are considered. The first is a circular area of radius R_o that is exposed to RF energy with uniform power density I_o. The second is a plane exposed to RF energy in a Gaussian pattern (approximating the exposure modeled in Colombi et al. 2015):

$$SAR = \frac{I_o T_{tr}}{\rho L} e^{-z/L} e^{-(r/Ro)^2} \qquad (9)$$
$$0 \le r < \infty$$

where I_o is the peak incident power density at the center of the irradiated area. In this case, the total absorbed power P is

$$P = \pi I_o T_{tr} R_o^2; \qquad (10)$$

i.e., the same as for the uniformly exposed disk of radius R_o.

There is apparently no closed form solution to the time-dependent BHTE for this two-dimensional (2D) case. However, the Green's function provides a simple closed form solution to steady state temperature (Gao et al. 1995). One assumes that an infinite medium absorbs power at a rate $I_o T_{tr}$ (W m^{-2}) in an infinitesimally thin layer centered in the plane (x,y,0). The steady state temperature increase T^{ss} (x,y,0) in the plane can be written as:

$$T^{ss}(x,y,0) = \frac{1}{4\pi k}\iint_D \frac{e^{-\sqrt{\frac{1}{R_1^2}\left[(x-x')^2+(y-y')^2\right]}}}{\sqrt{(x-x')^2+(y-y')^2}} I_0 T_{tr}(x',y')dx'dy' \quad (11)$$

where the integral extends over the entire heated area. This solution is derived from eqn (14) in Gao et al. (1995) from the Green's function for the BHTE for an infinite medium without assuming boundary conditions; i.e., the heat source is far from any boundary. By symmetry, eqn (11) also provides the surface temperature of an insulated half space of medium that is subject to surface heating at a rate $I_o T_{tr}$ (x,y), provided that it is multiplied by 2 to account for unidirectional flow of heat into the plane.

A closed form solution to eqn (11) is readily found for the two exposed disks:

$$T^{ss}_{uniform} = \frac{I_o T_{tr} R_1}{k}(1-e^{-x})\ \text{Uniformly irradiated area}$$
$$\mathrm{T}^{ss}_{Gaussian} = \frac{I_o T_{tr} R_0 \sqrt{\pi}}{2k} e^{x^2/4}(1-erf(x/2))\ \text{Gaussian beam pattern}$$
$$\text{where x} = \mathrm{R}_0/R_1. \qquad (12)$$

In the limit $R_o/R_1 \to \infty$, the maximum temperature in both cases becomes $I_o T_{tr} R_1/k$, which is the same as for the plane in the limit of short penetration depth (eqn 7a). In the opposite limit ($R_o/R_1 \to 0$), a series expansion yields

$$T^{ss}_{uniform} = \frac{I_o T_{tr} R_0}{k}\left(1-\frac{R_0}{2R_1}+\ldots\right)\ \text{Uniformly irradiated area}$$
$$\mathrm{T}^{ss}_{Gaussian} = \frac{I_o T_{tr} R_0}{k}\left(\frac{\sqrt{\pi}}{2}-\frac{R_0}{2R_1}+\ldots\right)\ \text{Gaussian beam pattern} \qquad (13\ \text{a, b})$$

Consequently, the asymptotic behavior for small R_o is independent of R_1 and consequently independent of the blood flow parameter m_b; it is simply the solution to the heat conduction equation. The transition between these limiting

cases occurs at $R_0 \approx R_1$ which defines the governing distance scale of the problem in the steady state (the governing distance in the transient regime is the shorter of R_1 and R_2).

Fig. 4a compares the analytical solutions for the maximum steady state temperature at the surface of the irradiated disk (which assume surface heating) with numerical simulations for a Gaussian beam pattern at 42 GHz with an energy penetration depth of 0.3 mm. The numerical and analytic solutions are very close, as expected given the short penetration depth of energy at that frequency. The time required to reach 90% of the steady state temperature (Fig. 4b) increases with beam diameter and reaches 10 min or more for irradiated areas with $R_0 > R_1$. From dimensional analysis, the characteristic time scale of the heat conduction problem is $R_o^2/\alpha \sim 16$ min for $R_o = 1$ cm, which is of the same magnitude as shown in Fig. 4b.

The Green's function solution can be extended for three dimensional heating. In addition, the Green's function for the time-dependent problem is also available (Gao et al. 1995). However, the convolution integral (that provides the temperature) would probably have to be obtained numerically for such cases, and a simpler approach might be direct numerical solution of the BHTE.

The Green's function in the (spatial) frequency domain provides a different perspective. The temperature increase in the frequency domain is the simple product of the Fourier

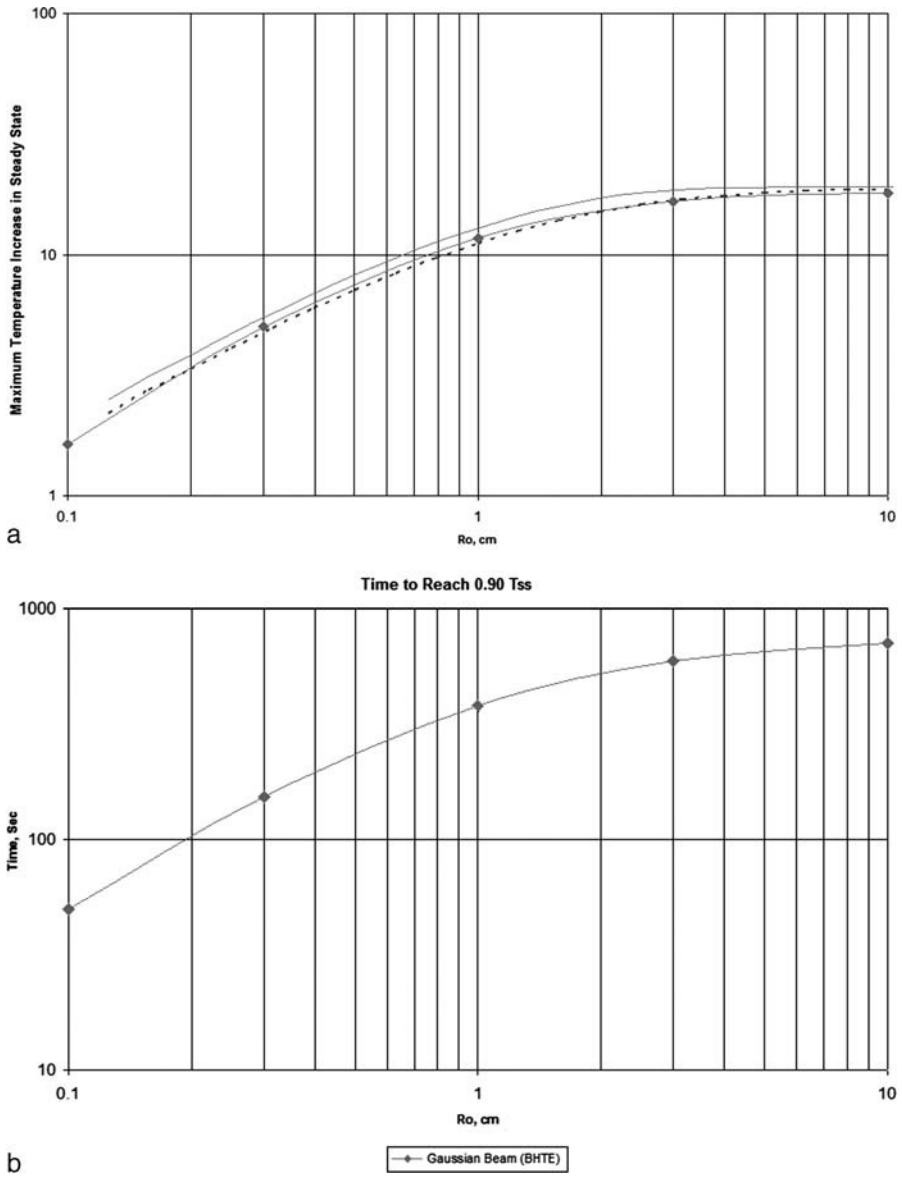

Fig. 4. (a) Maximum steady state temperature increase at surface of a disk of radius Ro subject to RF exposure with a Gaussian beam pattern, at absorbed power density at the surface (I_oT_{tr}) of 1000 W/m2 and frequency of 42 GHz. (♦) calculated by numerical solution of the BHTE, (_____) from analytical solution for exposed disk with uniform (Eq. 13(a)) and (----) Gaussian beam pattern (Eq. 13(b)). (b) Time required for maximum temperature to reach 90% of the increase in the steady state, calculated by numerical solution to the BHTE at 42 GHz with a Gaussian beam pattern.

transforms of the Green's function and source term and can be written (Gao et al. 1995):

$$T^{ss}(s) = \frac{1}{k}\,\frac{1}{s^2 + 1/R_1^2}\,Q(s) \qquad (14)$$

where $Q(s)$ and $T^{ss}(s)$ are the Fourier transforms of the heat input and temperature, and s is the spatial frequency. R_1 is given by eqn (8a). In engineering terms, eqn (14) describes a filtering operation with a second order lowpass filter that has two real poles at the spatial frequency $1/R_1$. Fluctuations in $Q(s)$ are strongly attenuated at spatial frequencies above $1/R_1$, falling off as the inverse square of the spatial frequency. In physical terms, this lowpass filtering is due to the effects of blood perfusion and thermal conduction, which smooth out the steady state temperature pattern over distances below R_1. The smoothing effect is stronger for smaller scale fluctuations in SAR.

Comparison with data

A search of the literature was conducted to identify papers that reported increases in skin temperature in humans produced by exposure to RF energy at or above 3 GHz, focusing on exposure levels that would be relevant to setting exposure limits (Table 1). Theoretical papers and modeling studies not reporting new data were not considered.

The literature that was located was quite limited. The most extensive body of data comes from a series of studies involving brief exposures to millimeter waves (usually 94 GHz) conducted to assess the safety of a military nonlethal weapons system (the Active Denial System) (Ryan et al. 2000). These studies involved high exposure levels that caused thermal pain within a few seconds and would have caused significant thermal damage if exposures had continued for much longer times. For short exposures (≈3 s), the temperature increase was closely predicted by a 1D heat conduction model using parameters similar to those in eqn (1) (Walters et al. 2000). A later study by the same group (Walters et al. 2004) considered longer exposures (up to 3–5 min) to human subjects and is discussed below.

In view of the paucity of data, a few additional studies were considered. Millenbaugh et al. (2006) exposed rats to high levels of millimeter wave energy for up to 1 h until death. Skin temperature increases from that study that were measured part way through those exposures are included in Table 1. In addition, Table 1 includes results from Adair et al. (2001) involving whole-body exposures to humans at 2.45 GHz for extended times (20 min) at levels exceeding exposure limits.

Three sets of data are considered in more detail.

a) Hendler et al. (1963) applied 10 GHz microwaves to the foreheads of four subjects for 2 min. The size of the irradiated area was not specified but apparently was several centimeters in diameter. Fig. 5 shows the calculated (BHTE) and measured temperature increase averaged over the four subjects, with the abscissa scaled as $t^{1/2}$. The thermal response shows an initial transient that transitions to $t^{1/2}$ response at longer times as expected from eqn (4a). The transition between the earlier and later parts of the transient response occurred at approximately τ_2 (36 s at 10 GHz) as expected from eqn (1). The results are in remarkable agreement with the simple model proposed here;
b) Alekseev and Ziskin (2003) and Alekseev et al. (2005) exposed the forearms and finger pads of human volunteers to millimeter waves at 42.25 GHz from an open waveguide placed near the body for up to 10 min exposure time. The radii of the exposed areas were 2.4 and 5.3 mm, and respective power densities were 2,080 and 549 W m^{-2}, respectively. For those exposures, the steady state temperature increase had been reached after 4–5 min (Fig. 6a, b). In these experiments, the temperature increase in the forearm agreed with the thermal model and was insensitive to the blood flow parameter. By contrast, the temperature increase in the finger pad was roughly one-half that in the forearm (Fig. 6a). In the finger pad, blood flow is approximately six times higher than in the forearm (Hertzman and Randall 1948). By eqn (6a), the steady state temperature increase would be smaller than for the forearm by a factor of $(6)^{1/2} \approx 2.4$, which is about what is observed. Equivalently, the governing distance R_1 is smaller by a factor of 2.4, and the steady state temperature increase has shifted from being conduction limited to perfusion limited. The authors conclude that in the forearm, the steady state increase in skin temperature is chiefly limited by heat conduction, while in the finger pad it is chiefly limited by blood perfusion; and
c) Walters et al. (2004) conducted an extensive series of experiments in which six subjects were exposed on their forearms to 94 GHz microwave energy with beam radius of 1.65 cm at two exposure levels (1,750 W m^{-2} for 2 or 8 min or 10^4 W m^{-2} for 4 s). The investigators measured skin blood flow using a laser Doppler flowmeter (which measures the velocity of erythrocytes in skin capillaries, not volumetric blood flow, as it appears in the BHTE). For the shorter exposures at higher power levels, the investigators reported only small effects when skin blood flow was reduced by occluding a blood pressure cuff placed on the arm.

In the experiments involving longer exposure times and lower power levels, the effects of skin blood flow were much more pronounced. After 3 min of exposure, the skin temperature had reached a plateau approximately 9 °C above baseline (pre-exposure) levels, while skin blood flow

Table 1. Summary of studies reporting temperature increases to skin from RF exposure.

Study	Frequency, power density	Radius of heated region, mm	Exposure time t, s	Measured skin temperature increase, °C	Max temperature increase after time *t* (numerical solution to BHTE, using parameters given in eq. 1)	Steady State Temperature increase (from shape factor approximation, eqn 13b) using parameters below eqn 1
Hendler et al. (1963)	10 GHz 2,500 W m^{-2} (quoted as power absorbed in skin)	(unspecified)	60	1	0.96	n/a
Alekseev and Ziskin (2005)	42.25 GHz, human forearm and finger, 2080 or 549 W m^{-2}	forearm 2.4 (2,080 W m^{-2}) 5.3 mm (549 W/m^2)	600	4.5 (forearm) 3.0	4.9 2.45	4.9 2.85
		Finger 2.4 (2,080 W m^{-2})	600	2.5	4.9	4.9
Nelson et al. (2002)	94 GHz, 1750 W m^{-2}	5 mm	180	8.4	8.8	10.2
Hu et al. (2011)	33.5 GHz, up to 8,530 W m^{-2}, mouse abdomen	3 mm	240	≈8	21	24
Gustrau and Bahr (2002)	77 GHz, 100 W m^{-2} (human forearm)	Not stated	Not stated (tens of min?)	0.7	1.2	n/a
Sasaki et al. (2014)	data at 40, 75 GHz, 2,000 W m^{-2} rabbit eye	6.5 mm (radius of cornea)	180 s	10.7 (40 GHz) (cornea) 13.2 (75 GHz) (cornea)	9.2 11.0 (calculations assume $m_b = 0$)	12.6 14.5
Walters et al. (2000)	94 GHz Back of 8 human subjects up to 18,000 W m^{-2} 3 s	2 cm	3 s	Up to 14 °C	Up to 14 °C (good agreement with 1D conduction model for 3 s exposures)	
Walters et al. (2004)	94 GHz, forearms of 6 human subjects "low power" 1,750 W m^{-2} (180 or 480 sec) "high power" 10^4 W m^{-2} (4 s) or	1.65 cm	180 or 480 s (low power) 4 s (high power)	Low power: 9 °C after 3 min (normal skin blood flow) 11 °C after 5 min (blood flow from times 180–300 sec reduced to approximately baseline (pre-exposure) value High power: 8 °C (small effect of blood flow)	BHTE simulations: 12.2 (with m_b given in eq. 1 11.1 (2 m_b) 10.2	n/a
Millenbaugh (2006)	Anesthetized rats 35GHz, 900 W m^{-2} 94 GHz, 750 W m^{-2} applied to shaved side of animals over an unstated area	8.5 cm (35 GHz) 6.7 cm (94 GH) (half power width)	Up to time of death (approximately 60 min total exposure time); skin temperature increases only considered in present analysis after first 10 min of exposure	≈8 °C (94 GHz) ≈ 10 °C (35 GHz)	8.3 7.8	n/a
Adair (2001)	Human back 2.45 GHz., 700 W/m^2	Large area	20 min	3.7	2.5	n/a

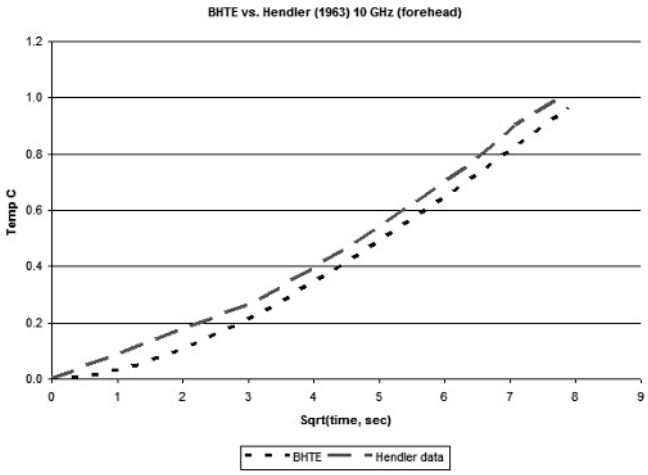

Fig. 5. Temperature increase in human forehead when exposed over an unstated area to RF energy at 10 GHz. Data from Hendler et al. (1963), calculations from BHTE, and using the 1D model and parameters assumed in the present study.

had increased twofold. The investigators then inflated a blood pressure cuff about the subject's arms (which reduced the skin blood flow to nearly its pre-exposure level) and continued exposure for an additional 2 min. The skin temperature then increased by an additional 2 °C.

It is simplest to compare the skin temperatures in the subjects with occluded skin blood flow to the model, since in both cases the blood perfusion remained at or near baseline (pre-exposure) levels. In those subjects, the skin temperature increased approximately 11 °C above baseline; the model predicted 12.2 °C. The time to approach the steady state increase in skin temperature (which was not reached in the experiments) was >100 seconds, compared to 300-400 sec from the model. In the exposed subjects, the skin blood flow was changing during the exposures, and the response time reflected those changes in a way consistent with the model.

Walters et al. (2004) is one of the few studies that measured the skin temperature increase under conditions where skin blood flow would be expected to be a major factor in limiting temperature rise. However, the RF exposure levels were far above any reasonable safety limit, being capable of causing pain after relatively brief exposures.

Finally, note that Adair et al. (2001) reported extended (20 min) exposures of human volunteers to RFR at 2.45 GHz. At that frequency, the energy penetration depth L is more than 1 cm, and the SAR pattern extends beyond skin into subcutaneous fat and muscle. The temperature increase predicted by the present model is similar to that observed by Adair et al. (2001).

One set of data conspicuously disagrees with the model (Hu et al. 2011), where the observed increase in skin temperature in a mouse abdomen after 4 min exposed to RF energy at 33.5 GHz was about one-half of the prediction of the model. The biological experiments in that study were not well described, and the skin blood flow in the animals is unknown.

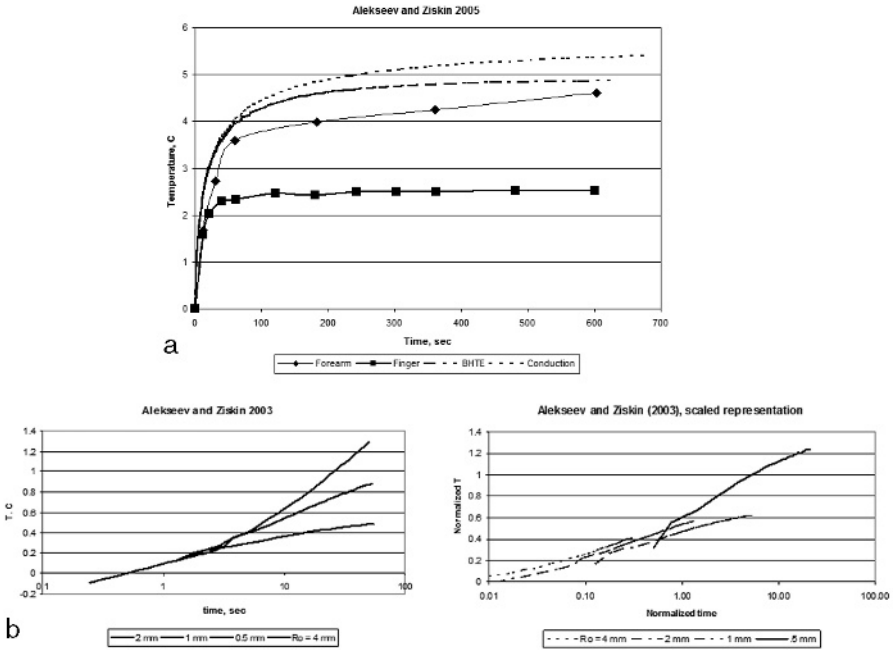

Fig. 6. (a) Temperature measured on forearm (♦) and finger (■) produced by 42.25 GHz with R_o = 0.24 cm, I_o = 2080 W m^{-2}. Also shown are calculated temperature increases for a Gaussian beam pattern for the heat conduction equation and BHTE. Data from Alekseev and Ziskin (2005). (b) Temperature increase in forearm, 42.25 GHz, 500 W m^{-2}. Radius of irradiated area ranges from 0.5 to 4 mm (data from Alekseev and Ziskin 2003). Fig. 6c. Same data as (b), with temperature scaled by $\pi I_o T_{tr} R_o/5\ k$ and time by R_o^2/α. The near convergence of the data on the scaled plot indicates that heat transfer is dominated by thermal conduction.

Going still farther afield, thermal damage to the eye is a recognized potential hazard of RF exposure that may well be the limiting hazard for design of standards for millimeter wave exposure. That topic would require a more extensive discussion than possible here, and it raises complexities in exposure assessment (including possible enhancement of SAR due to geometric resonances in the orbit) and effects of blood flow in the retina and other anatomic structures. However, two studies measured corneal temperature increases in animals exposed to RF exposure to the eye. These results are in reasonable to good agreement with the simple model presented here despite its grossly oversimplified nature. Foster et al. (2003) modeled the increase in temperature in the primate cornea after brief (1–5 s) exposure to 35 or 94 GHz microwave energy at high levels (20,000–70,000 W m^{-2}). A simple heat conduction model, using parameters similar to those assumed here, accurately fit the data with no adjustment in model parameters.

More recently, Sasaki et al. (2014) measured the temperature increase in rabbit corneas exposed to RF energy (40 and 75 GHz, 2,000 W m^{-2}) for 3 min. The results are in approximate agreement with the present model (Table 1). A previous study by that group (Hirata et al. 2006) subjected anesthetized and unanesthetized rabbits to 40–60 min exposures to the eye to 2.45 GHz radiation at an incident power density of 3,000 W m^{-2}. The authors developed a detailed, anatomically accurate, numerical simulation based on the BHTE and showed that anesthesia-induced changes in the thermoregulatory response of the animals resulted in approximately 9 °C higher temperatures in the vitreous cavity after extended (40–60 min) exposures. These were associated with reduced retinal blood flow in the anesthetized animals. These exposure levels would be far above any reasonable safety limit. In the unanesthetized animals, the resulting temperatures in the vitreous chamber exceeded 44 °C, which would have in all likelihood resulted in acute thermal injury to the eye, an endpoint that was not reported by the investigators.

DISCUSSION

The approximate thermal model developed here can be questioned on several accounts.

Validity of BHTE

The validity of the BHTE has been debated for many years; it is at best a continuum approximation for a decidedly complex situation. Initially, many investigators interpreted the perfusion parameter in the BHTE as referring to capillary perfusion, but it is now clear that heat exchange between tissue and blood mostly occurs in "thermally significant" vessels of 100 μm or more in diameter. A great many alternate formulations to the BHTE have been proposed, either continuum models using a variety of ad hoc approaches to model the effects of blood perfusion or models that attempt to include vascular architecture. However, theoretical work by Weinbaum et al. (1997) and Brinck and Werner (1995) showed that the BHTE is a good approximation for heat transfer in tissue provided that one adjusts its blood perfusion parameter by an "efficiency factor" in the range of 0.5–1 to account for thermal effects of countercurrent blood flow. Kolios et al. (1998) reported that the bioheat equation provided a good fit to the transient temperature rise near a buried heat source in tissue that was better than provided by alternate models considered in that study. While the BHTE does not account for short-range variations in temperature in the immediate vicinity of thermally significant blood vessels, modeling such effects would require detailed information about vascular architecture in the heated region, a major project in its own right.

Consequently, after many years of controversy, there is presently wide (but perhaps not universal) agreement that the BHTE is a reasonable model for heat transport in tissue provided that m_b is interpreted as an empirical parameter and not literally as a capillary perfusion rate (Baish 2015; Wissler 1998) or a quantity that is identical to that measured by the conventional Doppler flow meter. In any event, more rigorous models that include vessel-by-vessel analysis would require extensive tissue-specific information about vessel anatomy and microcirculation, which is not feasible for the general analysis attempted here.

Range of reported values for skin blood flow

A different uncertainty arises from the wide range of reported values of blood perfusion among subjects, as measured using different techniques and in different parts of the body. Table 2 summarizes different values of skin blood flow that have been reported in the literature, typically in the context of thermoregulation. The blood flow values have been converted to units commonly used in the physiological literature, mL of blood flow per kg of skin per minute (mL min^{-1} kg^{-1}) or on the basis of body surface area (mL min^{-1} cm^{-2}). Conversion to mL min^{-1} kg^{-1} was based on an assumed thickness of 2 mm and density of 1,109 kg m^{-3} resulting in 2.2 kg of skin per m^2 of body surface. The value of m_b used in the present model (equivalent to 106 mL min^{-1} kg^{-1}) is somewhat below the basal level (200 mL min^{-1} kg^{-1}) for skin quoted by Johnson and Kellogg (2010). However, reported values for skin blood flow in humans vary by factors of 2–4 or more depending on the part of the body in which it is measured and the measurement technique; there is also a lot of intersubject variability in measurements (Hertzman and Randall 1948).

Variability of skin blood flow with skin temperature

More so than in most tissues, skin blood flow is highly variable, reflecting the thermoregulatory function of skin.

Table 2. Reported values of skin blood flow.

Source	Skin blood flow	Comments
Williams and Leggett (1989)	120 mL/min^{-2}/kg^{-2}	Proposed reference value for resting human based on review of literature
Hasgall et al (2015) (values used for present model)	106 mL/min^{-2}/kg^{-2}	Value assumed in the present model
Hertzman and Randall (1948)	≈90 mL/min^{-2}/kg^{-2} (forearm) ≈ 770 mL/min^{-2}/kg^{-2} (finger pad) (average of two subjects)	Average of measurements in two subjects. Large variation in skin blood flow with location on body; large intersubject variability. Values from a photoelectric technique, authors say that values from thermal measurements are higher
Johnson and Kellogg (2010)	200 mL/min^{-2}/kg^{-2} basal conditions Falls to < 20 mL/min^{-2}/kg^{-2} with prolonged cooling of skin Increases to ≈ 3,000 mL/min^{-2}/1,000 g^{-1} with local heating up to 42 °C	"A nonlinear relationship of forearm blood flow to local skin temperature, such that increments in blood flow between 20 and 35 °C were relatively small, becoming much more dramatic above 37 °C, and reaching maximal or near maximal values at 42 °C"

Skin blood flow is chiefly determined by local skin temperature, but central thermoregulatory mechanisms play a role also as they regulate the transfer of heat from the body core through the skin to the environment. When skin is cooled below its normal level of about 34 °C or in cold environments, skin blood flow falls to levels as low as 20 mL min^{-1} kg^{-1}. In warm environments, skin blood flow increases due to vasodilation to reach levels as high as 3,000 mL min^{-1} cm^{-2} at a skin temperature of 42 °C (Johnson and Kellogg 2010).

However, effects from local heating of the skin may be different than those produced by environmental heating to the body where central thermoregulatory mechanisms become involved. The axon reflex type of vasodilatation only sets in above a threshold of about 39 °C (Margerl and Treede 1996), and increases in blood flow due to local heating of skin may be minor as long as skin temperature remains below that level. Experiments involving microwave exposure of small areas of skin have reported only modest increases in blood flow. For example, Walters et al. (2004) observed only twofold increases in skin blood flow during microwave exposure (94 GHz) to the forearm that raised the skin temperature by approximately 9 °C. Alekseev et al. (2005) "did not find any notable changes in [skin blood flow]" in their experiments involving exposures of the finger or forearm to 42.5 GHz microwaves resulting in a temperature increase of approximately 4 °C.

On the other hand, neglect of temperature-induced changes in blood flow can lead to astonishingly large errors in situations involving high levels of RF heating to large volumes of tissue. For example, Verhaart et al. (2014) reported that the BHTE with a fixed value of m_b (obtained from the same source as in the present model) predicted increases in brain temperature that were 30 °C above those measured in patients undergoing RF hyperthermia treatment for brain cancer. In the present study, neglect of a temperature-dependent increase in m_b would lead to an overestimate of temperature increase, but the errors are not expected to be high for the modest heating rates presently considered.

Background rates of heat flow across skin

A more accurate model would have to consider the background rates of heat flow across skin, which depend on environmental and physiological conditions and thermoregulatory status. These naturally occurring heat flows can be in the range of tens to hundreds of W m^{-2} for each of several mechanisms depending on environmental conditions and thermoregulatory status (Table 3). Because the experiments considered in Table 1 involved substantially higher power densities, they are not significant for present calculations, but they would be important to estimate temperature increases at the lower exposures allowed by exposure limits.

Against these uncertainties, one must consider the success of an early lumped-parameter model of the human

Table 3. Heat flows across the skin. Data from Stolwijk and Hardy (1977), ILO (2012), Fiala et al. (1999).

Mechanism	Typical ranges of heat flow (W m^{-2}) in skin of human
Cooling of skin by evaporation of sweat	Varies with environmental conditions, from 75 W m^{-2} (resting in thermoneutral environment) to > 350 W m^{-2} (strenuous exercise)
Convective cooling of skin	Depends on air flow, clothing. Approximately 2–4 W m^{-2} per K (20–40 W m^{-2} for a 10 °C difference between between skin and environment) in still air, to 10–15 W m^{-2} per K for forced convection with air velocity 1 m s.
Radiative cooling/heating of skin	Depends on clothing and radiant temperature of surroundings, approximately 5 W m^{-2} per K (approximately 50 W/m^2 for 10 °C difference between skin temperature and radiometric temperature of surroundings.
Conduction of heat from core into skin	20–100 W m^{-2} (depends on the thermoregulatory status, level of activity, clothing)

thermoregulatory system (Stolwijk and Hardy 1977) in accurately predicting thermal responses of human volunteers subjected to whole-body RF exposures at levels above present exposure limits with no adjustable parameters (Foster and Adair 2004). A theoretical formulation equivalent to the BHTE is used both in Stolwijk and Hardy (1977) and in a more recent thermal model for the human body (Fiala et al. 1999).

Overall, the simple model (eqn 1) is remarkably successful in accounting for thermal responses of tissue over a wide range of exposure conditions (Table 1). This is particularly impressive considering its extreme simplicity and lack of adjustment in its parameters. Reasons for this success include: (a) most of the studies reviewed in Table 1 involved irradiation over relatively small areas of body surface so that thermal conduction effects (which are essentially independent of physiological changes) predominated; (b) many of the exposures were of short duration so that the steady state was not reached (further increasing the relative importance of heat conduction vs. blood perfusion); and (c) the incident power densities were rather high, above rates of convective and radiative cooling of the skin, so that insulated boundary conditions are a good approximation. But even in the few cases where thermal effects of blood perfusion were likely to have been significant, the model predictions were generally in line with observations. More sophisticated, tissue-specific models might have provided better fits to the data, but then additional data would have been required to validate the models.

Comments on exposure limits. All three sets of exposure limits (IEEE 2005; ICNIRP 1998; FCC 2010) are presently under review for possible updating and revision. The limits are complex, with separate limits for occupational groups and the general public, and separate limits for exposure to unspecified areas of skin, as well as provisions for peak spatial exposure and time- and area-averaging provisions. Table 4 compares the basic restrictions in these three limits (for the general public), both for exposure to unspecified areas of the body and also spatial peak limits for exposures to limited areas of the body. (The present version of FCC limits does not distinguish between basic restrictions and reference levels and is expressed in terms of incident power density over the entire frequency range below 100 GHz.)

At microwave frequencies, all three limits are principally designed to protect against thermal hazards. Thus IEEE C95.1-2005 states that the partial body limits (which are most relevant to the present discussion) were designed "to protect against an excessive temperature rise in any part of the body that might result from localized or nonuniform exposure" (IEEE 2005). ICNIRP (1998) states that "between 10 and 300 GHz, basic restrictions are provided on power density to prevent excessive heating in tissue at or near the body surface."

Neither of these guidelines states precisely what constitutes "excessive heating" or "excessive temperature rise." Under realistic exposure conditions, the obvious thermal hazards from RF exposures to the skin and eye (thermal pain, burn, cataract) require increasing tissue temperature to 43–44 °C or more (considerably more, for realistic burn scenarios), although the possibility of thermal damage from extended exposures at lower temperatures cannot be excluded (Foster and Morrissey 2011). One might consider defining the basic restrictions in terms of a maximum allowable temperature increase above a baseline value, perhaps 1 °C, which would provide a nominal safety factor of about 10. That approach is intuitively attractive but would be difficult to implement with precision for a number of reasons. IEEE C95.1-2005 (p. 89) recognizes this problem: "Interpretation of the temperature data from modeling studies of the brain and eye must include consideration of the following limitations of the models: 1) the adequacy of physiological blood flow in many of the numerical model studies has not been verified, 2) none of the results for brain and eye have been validated in live animals and humans, and 3) the results from independent laboratories varied over a wide range. Until these limitations can be resolved, thermal models are useful but in and of themselves are not sufficient for safety standard development."

That limitation still exists today, and given the many variables (both environmental and physiological) that determine bioheat transfer, is unlikely to be remedied any time soon. Nevertheless, thermal models, even simple ones, can

Table 4. Basic restrictions for the general public above the transition frequencies specified by FCC, IEEE C95.1-2005, ICNIRP (1998) exposure limits. From Colombi et al. (2015).[a]

	FCC	ICNIRP (1998)	IEEE C95.1-2005
f_{tr} (GHz)	6	10	3
Power density limit (W m^{-2}) $f > f_{tr}$	10 (spatial peak)	10 (average over 20 cm^2)	10 ($f \leq$ 30 GHz average over 100/λ^2) ($f \geq$ 30 GHz average over 100 cm^2)
		100 (average over 1 cm^2)	18.56 $f^{0.699}$ ($f \leq$ 30 GHz, spatial peak) 200 ($f \geq$ 30 GHz, spatial peak)

[a] f_{tr} transition frequency, f frequency (GHz).

be useful in the design and evaluation of RF exposure limits by predicting (even if approximately) and comparing the heating of tissues under a wide range of exposure conditions. Specific uses might include:

1. Comparison of relative levels of protection of various limits: The three exposure limits (FCC, ICNIRP, IEEE C95.1-2005) for the general public are similar in terms of whole body exposures or partial body exposures over large body areas. However, the limits differ considerably in the "spatial peak" exposures (maximum power density at any location of skin) and definition of areas over which exposure is to be averaged.

All three limits have transitions at 3, 6, or 10 GHz (depending on the limit) as they change from SAR to incident power density as the principal dosimetric quantity. These were introduced chiefly for technical dosimetric reasons and have had unanticipated consequences. Colombi et al. (2015) showed that all three limits (IEEE, ICNIRP, FCC) implicitly result in discontinuities of as much as 7 dB in the allowable output power from an antenna mounted close to the body at the transition frequencies. The scaling properties of the BHTE suggest that similar differences will be present across the discontinuities in the guidelines, When the limits were last revised, there were few exposure scenarios in which people would operate antennas transmitting at these frequencies close to their bodies. That situation is about to change as new wireless technologies (5G) come into use in the near future;

2. Establishing spatial resolution needed in SAR calculations: Presently, compliance assessments for mobile phones and other transmitters that are used close to the body are chiefly done by physical measurements on "phantom" models of the body that are filled with tissue-equivalent fluids. This method is rapidly being replaced by numerical calculations of SAR using anatomically detailed models of the body. However, the cost and difficulty of such calculations increases quickly as the voxel size decreases. If the goal is to protect against thermal hazards, thermal scaling considerations can be used to establish the spatial resolution that would be needed for such calculations. Unless the exposure consists of very intense brief pulses (which is subject to different provisions of the guidelines), eqns (11) and (14) show that there is no need to worry about variations in the SAR over distance scales much smaller than R_1; the important quantity is the rate of surface heating and not the details of SAR distribution beneath the skin surface. Conceivably, such information may be important for very brief and intense pulses, although such exposures are seldom if ever encountered in the real world; and
3. Choice of temporal and spatial averaging volumes: The scaling properties of the BHTE discussed above can be used to help determine the spatial and temporal averaging to be incorporated into the limits. As Colombi et al. (2015) have noted, these limits are hardly optimal at present.

The scaling properties of the BHTE can help formulate averaging areas that are more consistent in their level of protection against thermal hazards across the frequency range considered here. In the BHTE, the characteristic distance over which a source of heat can affect tissue temperature is given by R_1. Eqn (11), in fact, defines an averaging process that could potentially be implemented directly in exposure limits. Given the uncertainties in the calculation, it would be adequate to simply average the exposure over an area of a few cm^2 of skin surface. Eqn (11) provides a clear basis to relax peak exposure values that occur in smaller areas, provided that the area-averaged exposure is maintained within fixed limits. The scaling principles discussed here also suggest that the exposure limits can be simplified. In the frequency range of present interest (>3–6 GHz), the absorbed power density at the skin surface (IoT_{tr}) is the chief dosimetric quantity that determines the increase in skin temperature.

CONCLUSION

1. Despite many years of research, few data exist on heating of human tissues by RF energy in the frequency range presently considered. The available studies have involved very few subjects, a very limited range of RF exposure parameters, and a limited number of body regions. The limitations in available data are striking in view of the fact that the exposure limits are designed to protect against thermal hazards. In addition, studies by Adair and colleagues on human thermoregulatory responses to RF energy (e.g., Adair and Black 2003) involving whole-body exposures also need to be extended to higher frequencies. Moreover, despite a few recent studies (e.g., measurements on ocular tissues by Sasaki et al. 2015), the extent of available data on dielectric properties of tissues above 20 GHz is quite limited, and such data are needed for numerical dosimetry studies. It is routine for scientists to call for "more data," but that need is really present for human exposures to RF energy in the frequency range presently considered.
2. The simple thermal model discussed here is surprisingly successful in predicting the thermal response in humans exposed to RF energy with no adjustment of model parameters. However, there are few data to test this or any other thermal model. The literature abounds with theoretical models for heating of skin, but rather few of them have been validated using data that are independent of those used to develop the models in the first place, and consequently their generalizability is uncertain.

3. This present study has shown that the scaling properties of the BHTE and heat conduction equations can be useful in synthesizing thermal response of skin to RF exposures over wide ranges. This approach has obvious application in the design and evaluation of safety limits for RF radiation, particularly when combined by more detailed numerical models.

Acknowledgment—This work was sponsored by Mobile Manufacturers Forum, which had no control over the contents of this paper.

REFERENCES

Adair E, Black D. Thermoregulatory responses to RF energy absorption. Bioelectromagnetics 24 (Supplement 6): S17–S38; 2003.

Adair E, Mylacraine K, Cobb B. Human exposure to 2,450 MHz CW energy at levels outside the IEEE C95.1 standard does not increase core temperature. Bioelectromagnetics 22: 429–439; 2001.

Alekseev S, Radzievsky A, Szabo I, Ziskin M. Local heating of human skin by millimeter waves: effect of blood flow. Bioelectromagnetics 26:489–501; 2005.

Alekseev S, Ziskin M. Local heating of human skin by millimeter waves: a kinetics study. Bioelectromagnetics 24: 571–581; 2003.

Andrews JG, Buzzi S, Choi W, Hanly SV, Lozano A, Soong AC, Zhang JC. What will 5G be? IEEE J Sel Areas Comm 32: 1065–1082; 2014.

Baish JW. Microvascular heat transfer. In: Bronzino JD, Peterson DR eds. Biomedical engineering handbook. New York: Wiley; 9.1–9.16; 2014.

Bhowmik A, Singh R, Repaka R, Mishra SC. Conventional and newly developed bioheat transport models in vascularized tissues: a review. J Therm Biol 38:107–125; 2013.

Brinck H, Werner J. Use of vascular and nonvascular models for the assessment of temperature distribution during induced hyperthermia. International J Hyperthermia 11: 615–626; 1995.

Colombi D, Thors B, Tornevik C. Implications of EMF exposure limits on output power levels for 5G devices above 6 GHz. IEEE Antennas Wirel Propag Lett 14:1247–1249; 2015.

Federal Communications Commission. Code of Federal Regulations CFR title 47, part 1.1310. 2010.

Fiala D, Lomas KJ, Stohrer M. A computer model of human thermoregulation for a wide range of environmental conditions: the passive system. J Appl Physiol 87:1957–1972; 1999.

Foster KR, D'Andrea J, Chalfin S, Hatcher D. Thermal modeling of millimeter wave damage to the primate cornea at 35 GHz and 94 GHz. Health Phys 84:764–769; 2003.

Foster KR, Glaser R. Thermal mechanisms of interaction of radiofrequency energy with biological systems with relevance to exposure guidelines. Health Phys 92:609–620; 2007.

Foster KR, Lozano-Nieto A, Riu P. Heating of tissues by microwaves: a model analysis. Bioelectromagnetics 19: 420–428; 1998.

Foster KR, Adair ER. Modeling thermal responses in human subjects following extended exposure to radiofrequency energy. Biomed Eng Online 3:4; 2004.

Foster KR, Kritikos HN, Schwan HP. Effect of surface cooling and blood flow on the microwave heating of tissue. IEEE Trans Biomed Eng 25:313–316; 1978.

Foster KR, Morrissey JJ. Thermal aspects of exposure to radiofrequency energy: report of a workshop. Int J Hypertherm 27: 307–319; 2011.

Gabriel S, Lau RW, Gabriel C. The dielectric properties of biological tissues: III. Parametric models for the dielectric spectrum of tissues Phys Med Biol 41:2271–2293; 1996.

Gao B, Langer S, Corry PM. Application of the time-dependent Green's function and Fourier transforms to the solution of the bioheat equation. Int J Hypertherm 11:267–285; 1995.

Gustrau F, Bahr A. W-band investigation of material parameters, SAR distribution, and thermal response in human tissue. IEEE Trans Microwave Theory Tech 50:2393–2400; 2002.

Hasgall PA, Di Gennaro F, Baumgartner C, Neufeld E, Gosselin MC, Payne D, Klingenböck A, Kuster N. IT'IS Database for thermal and electromagnetic parameters of biological tissues, Version 2.6 [online]. 2015. Available at ***www.itis.ethz.ch/database***. Accessed 20 August 2015.

Hendler E, Hardy JD, Murgatroyd D. Skin heating and temperature sensation produced by infrared and microwave irradiation. Temperature 3:211–230; 1963.

Hertzman A, Randall W. Regional differences in the basal and maximal rates of blood flow in the skin. J Appl Physiol 1: 234–241; 1948.

Hirata A, Watanabe S, Kojima M, Hata I, Wake K, Taki M, Sasaki K, Fujiwara O, Shiozawa T. Computational verification of anesthesia effect on temperature variations in rabbit eyes exposed to 2.45 GHz microwave energy. Bioelectromagnetics 27: 602–612; 2006.

Hu S, Fan C, Yang L, Sun F, Kou WA. Thermal model for heating of rat skin by millimeter waves Fourth International Workshop on Advanced Computational Intelligence. Hubei, China: Wuhan; 2011:447–451. Available online at ***http://ieeexplore.ieee.org/document/6160048/***. Accessed on 6 October 2016.

International Commission on Non-Ionizing Radiation Protection. Guidelines for limiting exposure to time-varying electric, magnetic, and electromagnetic fields (up to 300 GHz). Health Phys 74:494–522; 1998.

Institute of Electrical and Electronics Engineers. Standard for safety levels with respect to human exposure to radio frequency electromagnetic fields, 3 kHz to 300 GHz. Piscataway, NJ: IEEE; IEEE C95.1; 2005.

Institute of Electrical and Electronics Engineers. Standard for safety levels with respect to human exposure to radio frequency electromagnetic fields, 3 kHz to 300 GHz. Amendment 1: specifies ceiling limits for induced and contact current, clarifies distinctions between localized exposure and spatial peak power density. Piscataway, NJ: IEEE; IEEE C95.1a; 2010.

International Labor Office. Encyclopedia of occupational health and safety, Chapter 42 [online]. 2012. Available at ***www.ilocis.org/en/contilo.html***. Accessed 17 July 2016.

Johnson JM, Kellogg DL Jr. Local thermal control of the human cutaneous circulation. J Appl Physiol 109:1229–1238; 2010.

Kanezaki A, Hirata A, Watanabe S, Shirai H. Parameter variation effects on temperature elevation in a steady-state, one-dimensional thermal model for millimeter wave exposure of one-and three-layer human tissue. Phys Med Biol 55: 4647–4659; 2010.

Kolios M, Worthington A, Sherar M, Hunt J. Experimental evaluation of two simple thermal models using transient temperature analysis. Phys Med Biol 43:3325–3340; 1998.

Margerl W, Treede R-D. Heat-evoked vasodilatation in human hairy skin: Axon reflexes due to low-level activity of nociceptive afferents. J Physiol 497:837–848; 1996.

Millenbaugh N, Kiel J, Ryan K, Blystone R, Kalns J, Brott B, Cerna C, Lawrence W, Soza L, Mason P. Comparison of blood pressure and thermal responses in rats exposed to

millimeter wave energy or environmental heat. Shock 25: 625–632; 2006.
Nelson D, Walters T, Ryan K, Emerton K, Hurt W, Ziriax J, Johnson L, Mason P. Inter-species extrapolation of skin heating resulting from millimeter wave irradiation: modeling and experimental results. Health Phys 84:608–615; 2003.
Pennes H. Analysis of tissue and arterial blood temperatures in the resting human forearm. J Appl Physiol 1:93–122; 1948.
Riu P, Foster K, Blick D, Adair E. A thermal model for human thresholds of microwave-evoked warmth sensations. Bioelectromagnetics 18:578–583; 1997.
Ryan K, D'Andrea J, Jauchem J, Mason P. Radio frequency radiation of millimeter wave length: potential occupational safety issues relating to surface heating. Health Phys 78: 170–181; 2000.
Sasaki K, Sakai T, Nagaoka T, Wake K, Watanabe S, Kojima M, Hasanova N, Sasaki H, Sasaki K, Suzuki Y, Taki M, Kamimura Y, Hirata A, Shirai H. Dosimetry using a localized exposure system in the millimeter-wave band for in vivo studies on ocular effects. IEEE Trans Microwave Theory Tech 62: 1554–1564; 2014.
Stolwijk JAJ, Hardy JD. Control of body temperature. In: Douglas HK, ed. Handbook of physiology, section 9, reactions to environmental agents. Bethesda, MD: American Physiological Society; 1977:45–69.
Verhaart RF, Rijnen Z, Fortunati V, Verduijn GM, van Walsum T, Veenland JF, Paulides MM. Temperature simulations in hyperthermia treatment planning of the head and neck region. Rigorous optimization of tissue properties Strahlentherapie Und Onkologie 190:1117–1124; 2014.
Walters T, Blick D, Johnson L, Adair E, Foster K. Heating and pain sensation produced in human skin by millimeter waves: comparison to a simple thermal model. Health Phys 78: 259–267; 2000.
Walters T, Ryan K, Nelson D, Blick D, Mason P. Effects of blood flow on skin heating induced by millimeter wave irradiation in humans. Health Phys 86:115–120; 2004.
Weinbaum S, Xu L, Zhu L, Ekpene A. A new fundamental bioheat equation for muscle tissue. 1. Blood perfusion term. J Biomechanical Eng Trans Asme 119:278–288; 1997.
Williams L, Leggett R. Reference values for resting blood-flow to organs of man. Clin Phys Physiol Meas 10:187–217; 1989.
Wissler E. Pennes' 1948 paper revisited. J Appl Physiol 85: 35–41; 1998.
Xu F, Lu TJ, Seffen KA, Ng EYK. Mathematical modeling of skin bioheat transfer. Appl Mech Rev 62:050801; 2009.
Yeung C, Atalar E. A Green's function approach to local RF heating in interventional MRI. Med Phys 28:826–832; 2001.

■■